JOURNAL OF BACTERIOLOGY, June 1997, p. 3691–3696 Vol. 179, No. 11
0021-9193/97/$04.00+0

Characterization of a Thermosensitive *Escherichia coli* Aspartyl-tRNA Synthetase Mutant

FRANCK MARTIN,[1] GARY J. SHARPLES,[2] ROBERT G. LLOYD,[2] SYLVIA EILER,[3] DINO MORAS,[3] JEAN GANGLOFF,[1] AND GILBERT ERIANI[1]*

UPR 9002, Structure des Macromolécules Biologiques et Mécanismes de Reconnaissance, CNRS, Institut de Biologie Moléculaire et Cellulaire, 67084 Strasbourg,[1] and UPR 9004, Laboratoire de Biologie Structurale, IGBMC, CNRS/INSERM/ULP, 67404 Illkirch,[3] France, and Department of Genetics, University of Nottingham, Queens Medical Center, Nottingham NG7, United Kingdom[2]

Received 11 November 1996/Accepted 27 February 1997

The *Escherichia coli tls-1* strain carrying a mutated *aspS* gene (coding for aspartyl-tRNA synthetase), which causes a temperature-sensitive growth phenotype, was cloned by PCR, sequenced, and shown to contain a single mutation resulting in substitution by serine of the highly conserved proline 555, which is located in motif 3. When an *aspS* fragment spanning the codon for proline 555 was transformed into the *tls-1* strain, it was shown to restore the wild-type phenotype via homologous recombination with the chromosomal *tls-1* allele. The mutated AspRS purified from an overproducing strain displayed marked temperature sensitivity, with half-life values of 22 and 68 min (at 42°C), respectively, for tRNA aminoacylation and ATP/PP_i exchange activities. K_m values for aspartic acid, ATP, and $tRNA^{Asp}$ did not significantly differ from those of the native enzyme; thus, mutation Pro555Ser lowers the stability of the functional configuration of both the acylation and the amino acid activation sites but has no significant effect on substrate binding. This decrease in stability appears to be related to a conformational change, as shown by gel filtration analysis. Structural data strongly suggest that the Pro555Ser mutation lowers the stability of the Lys556 and Thr557 positions, since these two residues, as shown by the crystallographic structure of the enzyme, are involved in the active site and in contacts with the tRNA acceptor arm, respectively.

The aminoacyl-tRNA synthetases (aaRS) are a family of enzymes which play a crucial role in maintenance of the translation fidelity of the genetic message into proteins: in a two-step reaction, they catalyze the esterification of an amino acid to the 2′- or 3′-hydroxyl group of the 3′-terminal adenosine of the cognate tRNA. These enzymes are believed to be among the earliest proteins to have arisen, and their evolutionary history is closely associated with the development of the genetic code. Despite their similar substrates and mechanisms of action, aaRS present remarkable diversity in terms of size, amino acid sequence, subunit size, and quaternary organization. However, based on mutually exclusive sets of sequence motifs and catalytic domain structures, aaRS could be partitioned into two distinct classes (4, 6). Class I enzymes are characterized by a catalytic domain corresponding to a Rossmann nucleotide binding fold (14); it contains the two signature peptides, HIGH (18) and KMSKS, which are involved in catalysis and substrate binding (10). Class II displays a peculiar folding topology as the core design of its active site region; it consists of a six-stranded antiparallel β-sheet flanked by two α-helices (4, 15). Three signature motifs common to this class are present in this domain. The class partition also correlates with a catalytic difference in the primary site attachment of the amino acid to the 3′ end of the tRNA; all class I aaRS attach their amino acids to the 2′-hydroxyl group, whereas class II aaRS (with the exception of PheRS) bind their amino acids to the 3′-hydroxyl group of the ribose of the terminal adenosine (6).

Structure-function studies of these enzymes benefit from the combination of genetic, biochemical, and structural approaches. Site-directed mutagenesis is an efficient and convenient method largely used to evaluate the function of any residues in the protein. Specific domains, such as amino acid binding sites, may be investigated, as was done in the case of PheRS (11), SerRS (19), and ArgRS from *Escherichia coli* (8) by characterization of mutant strains resistant to amino acid analogs. Another valuable strategy for identifying functional elements involved in catalysis is selection and analysis of mutations in aaRS, leading to an auxotrophic or temperature-sensitive phenotype; in addition, these conditional mutants may afterward be used in genetic systems to screen for functional elements of enzymes.

Some years ago, a mutant of *E. coli* K-12, a *tls-1* mutant, that exhibited a temperature-sensitive growth phenotype in low-salt media was identified (16, 17). DNA fragments alleviating the temperature sensitivity of a *tls-1* strain (CS143) were cloned and sequenced. This revealed that the *tls-1* mutation was an allele of *aspS*, the gene coding for aspartyl-tRNA synthetase (7), and was located in the DNA part coding for the carboxy terminus of AspRS (16). In this study, we characterized the *tls-1* mutation by PCR amplification, cloning, and sequencing and analyzed the kinetic properties of the corresponding mutated AspRS. Furthermore, we established that restoration of the wild-type phenotype of CS143 by plasmid DNA encoding a C-terminal region of AspRS (16) was not effected by the corresponding expressed protein but relied on a double homologous recombination event.

* Corresponding author. Mailing address: UPR 9002, Structure des Macromolécules Biologiques et Mécanismes de Reconnaissance, CNRS, Institut de Biologie Moléculaire et Cellulaire, 15, rue René Descartes, 67084 Strasbourg, France. Phone: 03.88.41.70.42. Fax: 03.88.60.22.18. E-mail: eriani@ibmc.u-strasbg.fr.

MATERIALS AND METHODS

Bacterial strains, media, and growth conditions. *E. coli* was grown in Luria-Bertani (LB) medium or in low-salt LB medium (0.5 g of NaCl per liter) containing ampicillin at 50 μg/ml when required. *E. coli* AB1157 [F^- *thi-1 hisG4*

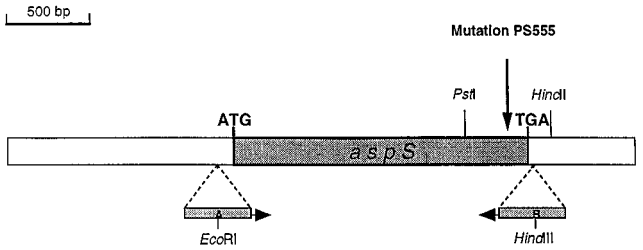

FIG. 1. Map of the DNA fragment containing the gene coding for *aspS* [or *aspS* (*tls-1*)]. The positions of the upstream (A) and downstream (B) priming oligonucleotides for PCR with their respective cloning restriction sites (*Eco*RI and *Hin*dIII) are shown. The arrow on the *Pst*I-*Hin*cII fragment [called *C* or *C* (*tls-1*) if mutated] indicates position 1663, which, after mutation from C to T, results in replacement of proline with serine; this fragment was ligated into pBluescriptII SK$^+$ 96 nucleotides downstream of the initiation codon and in frame with the gene coding for β-galactosidase to obtain pBluescriptII SK$^+$ *C* or *C* (*tls-1*) [p*aspS-C* or *C* (*tls-1*)].

Δ(*gpt-proA*)*62 argE3 thr-1 leuB6 kdgK51 rfbD1 ara-14 lacY1 galK2 xyl-5 mtl-1 supE44 tsx-33 rpsL31* (1)] was grown at 37 or 42°C in low-salt LB medium, whereas *E. coli* CS143 (strain isogenic to AB1157, carrying the *tls-1* mutation) was grown at 30°C in the same medium. Growth rates were determined in thermostated spectrophotometer cuvettes containing 1.6 ml of medium (stirred with a magnet bar) by continuous measurement of absorbance at 700 nm in a Kontron Uvikon spectrophotometer.

Characterization of the *tls-1* mutation by PCR cloning and sequencing. DNAs from strains AB1157 and CS143 were obtained from single colonies suspended in 50 μl of sterilized distilled water, with vigorous shaking for 3 min followed by incubation at 37°C for 15 min. Two microliters of this mixture was used as a DNA template in the PCR. The reaction mixture also contained 100 mM Tris-HCl (pH 8.3), 100 mM $MgCl_2$, 200 mM KCl, 0.75 mM each deoxynucleoside triphosphate, 1 U of *Taq* DNA polymerase, and 1 μM each oligonucleotide primers 5′ GGC GTAGAGTCTGAATTCAGGCCCGATATA 3′ and 5′ GTGTATTTGAAGC TTATCAGTTATTCTCAG 3′ that flanked the *aspS* gene and which contained an *Eco*RI site and a *Hin*dIII restriction site (underlined), respectively. The reaction mixture was transferred to a programmable heating block (Dry-Block; Osi), which was heated to 92°C for 1 min to denature the genomic DNA and then to 50°C for 1 min for primer annealing; primer extension steps were performed at 72°C for 2 min. The denaturation-annealing-extension cycle was repeated 25 times under the same conditions. The PCR products were fractionated on a 0.8% agarose gel. The 1.9-kb fragments corresponding to the expected size between the primer annealing sites flanking the *aspS* gene were cut out of the gel and purified with Geneclean II. These fragments were cut at their *Eco*RI and *Hin*dIII sites and cloned into the corresponding restriction sites of the polylinker of pBluescriptII SK$^+$. Recombinant plasmids were sequenced with appropriate oligonucleotides derived from the wild-type *aspS* DNA sequence. The C-terminal fragments of the *aspS* and *aspS* (*tls-1*) genes were subcloned as 496-bp *Pst*I-*Hin*cII DNA fragments (from +1379 to +1875) between the *Pst*I and *Sma*I sites of pBluescriptII SK$^+$.

Purification and kinetic properties of the mutated Pro555Ser AspRS. The mutated Pro555Ser enzyme was overproduced in strain CS143 from p*aspS*(*tls-1*). The crude extract from a 500-ml culture of the transformant strain grown at 37°C in LB medium (100-μg/ml ampicillin) up to an optical density at 700 nm (OD_{700}) of 2 was prepared as previously described (14). After centrifugation at 105,000 × *g* for 120 min, the extract (about 35% of the protein was the Pro555Ser AspRS) was dialyzed overnight at 4°C against 50 mM Tris-HCl (pH 8)–0.1 mM EDTA–1 mM $MgCl_2$–5 mM β-mercaptoethanol–20% glycerol (buffer A). The Pro555Ser protein was purified from other proteins in one step by high-performance liquid chromatography (HPLC) on a TSK 2SW DEAE column (diameter, 4.6 mm; height, 250 mm). About 20 mg of crude extract proteins was loaded at a time on a column previously equilibrated with a solution containing 93% 20 mM potassium phosphate (pH 7.5) and 7% 1 M potassium phosphate (pH 6.5). After a 15-ml wash with the latter buffer, elution was carried out by linearly increasing the 1 M potassium phosphate (pH 6.5) to 25% over 30 min. The flow rate throughout was 1 ml/min. Fractions presenting AspRS activity were pooled and dialyzed against buffer A containing 60% (vol) glycerol. Wild-type AspRS was purified by the same protocol, except that overproduction was performed for strain AB1157 transformed by p*aspS*. After these steps, both proteins appeared homogeneous on sodium dodecyl sulfate-polyacrylamide gel electrophoresis gels.

The aminoacylation activity of the purified enzymes was assayed by adding 10 μl of the appropriately diluted enzyme solution to 90 μl of the following reaction mixture: 100 mM Tris-HCl (pH 7.5)–30 mM KCl–10 mM ATP–22 mM $MgCl_2$–5 mM glutathione–0.1-mg/ml bovine serum albumin–0.1 mM [^{14}C]aspartic acid (25,000 dpm/nmol)–10-mg/ml unfractionated *E. coli* tRNA. At constant time intervals of incubation at 37°C, 20 μl of the reaction mixture was assayed for [^{14}C]aspartyl-tRNA^{Asp} by the method previously described (13), and initial rates were determined. The K_m values for aspartic acid, ATP, and tRNA^{Asp} in the aminoacylation reaction were determined by varying the concentration of the assayed substrate over a 10-fold range.

The AspRS activity in the amino acid activation step was measured by the ATP/PP_i exchange rate. The reaction mixture (100 μl) contained 100 mM HEPES (sodium salt) (pH 7.2), 10 mM $MgCl_2$, 2 mM [^{32}P]PP_i (1 to 2 cpm/pmol), 2 mM ATP, 10 mM aspartic acid, and 10 mM KF. The reaction was started by enzyme addition, and after various incubation times at 37°C, 50 μl was removed and measured for synthesized [^{32}P]ATP, treated, and counted as described elsewhere (12).

RESULTS AND DISCUSSION

Analysis of the mutated *aspS* gene by PCR, cloning, and sequencing. DNAs from the mutated strain CS143 and the control strain AB1157 were prepared and subjected to PCR amplification to isolate the *aspS* (*tls-1*) mutation (Fig. 1) (see Materials and Methods). Sequencing of the cloned PCR products revealed that the DNA of *aspS* (*tls-1*) differed from the wild-type *aspS* by a single mutation which was located, as previously established (16), in the *aspS* region coding for the C-terminal part of the protein. It consisted of a replacement of C1663 with a T, resulting in replacement of the conserved proline 555 of motif 3 with serine.

Growth of the *tls-1* strain and derivatives transformed by plasmidic forms of *aspS*, *aspS* (*tls-1*), and a C-terminal fragment of *aspS* or *aspS* (*tls-1*). The growth rates of bacterial cells were determined by continuous absorbance measurements in thermostated cuvettes (see Materials and Methods). All cultures were started by inoculating the medium with an overnight culture to an OD_{700} of 0.045. As shown in Fig. 2, the linear growth rate (ΔOD per hour) of the *tls*$^+$ AB1157 strain at 42°C in low-salt LB medium is about 0.3/h, whereas growth of CS143 (AB1157*tls-1*) reaches a OD_{700} plateau of about 0.3 already after a 3-h incubation period (Fig. 2). This plateau effect disappeared when incubation was at 30°C, linear growth rates being in that case 0.12/h and 0.21/h, respectively, for CS143 and AB1157 (data not shown). Suppression of the temperature-sensitive phenotype restoring growth rate to a level corresponding to those of the *tls*$^+$ control strain AB1157 is obtained by transformation of CS143 with multicopy pBluescriptII SK$^+$ containing either *aspS* or, surprisingly, *aspS* (*tls-1*) [p*aspS* and p*aspS*(*tls-1*), respectively] (Fig. 2). Clearly, the mutated AspRS retains some activity at 42°C, as shown by the ability of *aspS* (*tls-1*) to compensate for the temperature-sensitive phenotype at a high gene dosage.

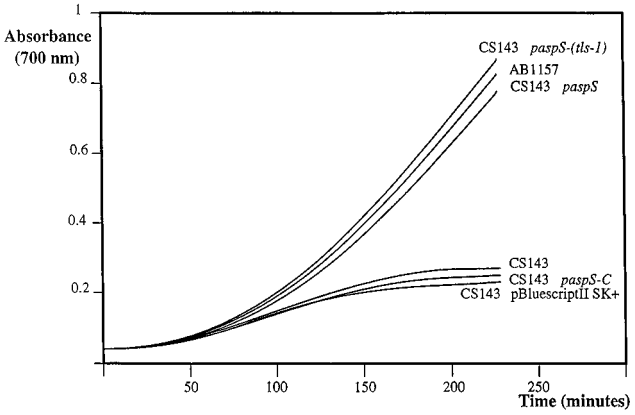

FIG. 2. Growth at 42°C in low-salt LB medium of the *tls*$^+$ and *tls-1* strains (AB1157 and CS143, respectively) and their transformants containing pBluescriptII SK$^+$, p*aspS*, p*aspS*(*tls-1*), and p*aspS-C*. At time zero, 1.6-ml samples of low-salt medium were inoculated from an overnight culture in LB medium at 30°C to an A_{700} of 0.045, and growth was monitored by continuous measurement of A_{700} throughout the period indicated.

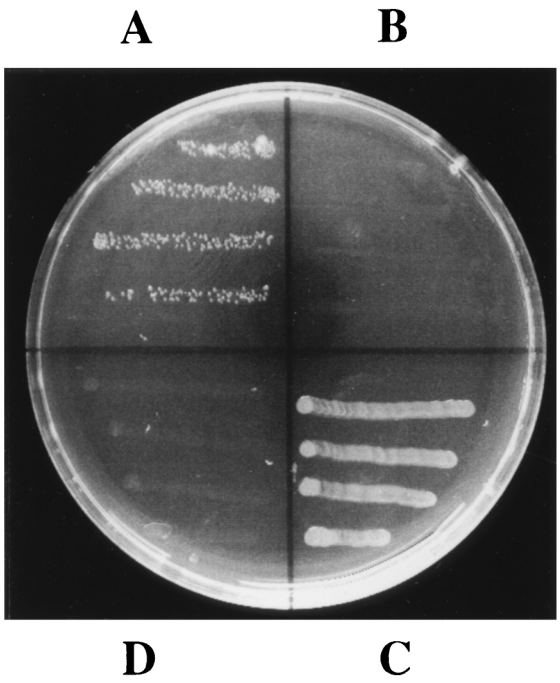

FIG. 3. Growth properties of the CS143 strain transformed by p*aspS-C* (A), pBluescriptII SK$^+$ (B), p*aspS*(*tls-1*) (C), and p*aspS-C*(*tls-1*) (D) on low-salt LB plates at 42°C. A single colony corresponding to each of the different transformants grown at 30°C on LB plates containing ampicillin was picked to inoculate 1 ml of LB broth containing ampicillin. After overnight incubation at 30°C, 10 μl from each sample was streaked on a low-salt LB plate containing ampicillin, and the plate was incubated for 1 day at 42°C.

Whether a higher degradation rate or lower activity of the mutated enzyme at 42°C is responsible for the growth-limiting AspRS activity within CS143 remains to be established. Concerning the previously mentioned temperature-sensitive phenotype complementation (16) by the C-terminal 496-bp *Pst*I-*Hin*cII fragment from *aspS* (*aspS-C*), complementation was not observed within the 3-h period during which growth was monitored (see the curve corresponding to p*aspS-C* in Fig. 2). A significant increase in OD appeared only after 6 to 8 h of incubation of CS143 transformed by p*aspS-C*. This behavior will be examined below. Noticeably, no restoration of CS143 cell viability was obtained in the presence of p*aspS-C*(*tls-1*) [p*aspS-C*(*tls-1*) contains the C-terminal 496-bp *Pst*I-*Hin*cII fragment from *aspS* (*tls-1*)].

Complementation of CS143 by *aspS-C* is due to double homologous recombination with chromosomal *aspS* (*tls-1*). As mentioned before, Sharples and Lloyd and Shurvington et al. (16, 17) showed that pUC18 carrying a fragment encoding the C-terminal region of AspRS (*aspS-C*) complements the temperature-sensitive phenotype of CS143. At first glance, this appeared to be clear evidence that the C-terminal region of AspRS either alone or in a heterodimeric association with the mutated AspRS monomer possessed some activity. However, since the C-terminal fragment lacked domains essential for catalysis, preference was given to the hypothesis of the active heterodimer (16). In fact, all of our attempts failed to isolate this heterodimer from a CS143 transformant cooverproducing the Pro555Ser-mutated AspRS and the C-terminal fragment of AspRS. However, we noticed that the growth rate curve at 42°C of the CS143-p*aspS-C* transformant in liquid low-salt LB medium was quite similar, in a first stage, to the growth rate of CS143 (Fig. 2). Complementation appeared only after a 6- to 8-h incubation time. In addition, it was observed that when the CS143-p*aspS-C* transformant was incubated for 18 h at 42°C on low-salt LB agar plates containing ampicillin (conditions under which complementation has been observed), the bacterial lawn observed was not uniform but was composed of separate colonies (Fig. 3). Bacteria from these colonies displayed a *tls*$^+$ phenotype at 42°C on low-salt LB agar plates (data not shown) as well as in low-salt LB broth. This was clear evidence that complementation of the thermolabile phenotype of CS143 by p*aspS-C* resulted from homologous recombination between the chromosomal *aspS* (*tls-1*) and the plasmid C-terminal fragment. This was confirmed by sequencing the genomic *aspS* DNAs of the revertant cells (prepared by PCR, as previously described), which showed that they were identical to the wild-type *aspS* gene having a proline at position 555. Lastly and as expected, the p*aspS-C*(*tls-1*) plasmid encoding the C-terminally mutated fragment was unable to compensate for the temperature-sensitive phenotype of CS143.

Kinetic analysis of the mutated Pro555Ser protein. Mutated Pro555Ser AspRS and native AspRS were overproduced and purified, and their kinetic parameters were determined as described in Materials and Methods.

First, it was observed that the acylation activity of the mutated AspRS differed from one preparation to another and decreased over time with storage. In none of the cases did the enzymes display more than 45% of the wild-type enzyme activity (18 s^{-1}) after purification (Table 1). This instability was demonstrated by comparing the thermal stability of Pro555Ser-mutated AspRS to that of the native enzyme. The proteins were incubated at 42°C, and after various time intervals, aliquots were tested both for ATP/PP_i exchange and for aminoacylation activity. The aminoacylation activity of the mutated enzyme decreased in a monomolecular reaction mode and was reduced by half after 22 min of incubation, whereas the wild-type enzyme retained its full activity during this time interval (Fig. 4). Noticeably, ATP/PP_i exchange was also inactivated at 42°C, although with a rate about threefold lower than that of acylation (Fig. 4). The existence of different rates suggests that inactivation of the two catalytic steps proceeds by two separate processes. Assuming that they occur by an ordered mechanism, this would imply that acylation is abolished first and at a rate higher than that of the ATP/PP_i exchange activity. Concerning the first-order reaction mode of the activity decrease (ending in a completely inactive enzyme), this typically indicates that inactivation is occurring in a one-step process consisting of a shift of the enzyme from its fully active state to an inactive state. Thus, a decrease in activity would in fact reflect the decrease in concentration of the active enzyme species. As shown in Table 1, mutation Pro555Ser had no effect on K_m values for tRNA, ATP, and aspartic acid. These parameters indeed corresponded to those of the active form of the enzyme, K_m values for the inactive species being unmeasurable. The

TABLE 1. Kinetic parameters for aminoacylation reactions[a]

Enzyme	k_{cat} (s^{-1})	K_m (μM)		
		ATP	Asp	$tRNA^{Asp}$
Native AspRS	18	90	60	0.6
Pro555Ser (45%)	8	95	70	ND
Pro555Ser (11%)	2	80	50	0.5

[a] Parameters for AspRS and two Pro555Ser enzymes having 45 and 11% acylation activity (as indicated) compared to that for the wild-type enzyme were determined. k_{cat} values for saturating concentrations of aspartic acid were calculated. ND, not determined.

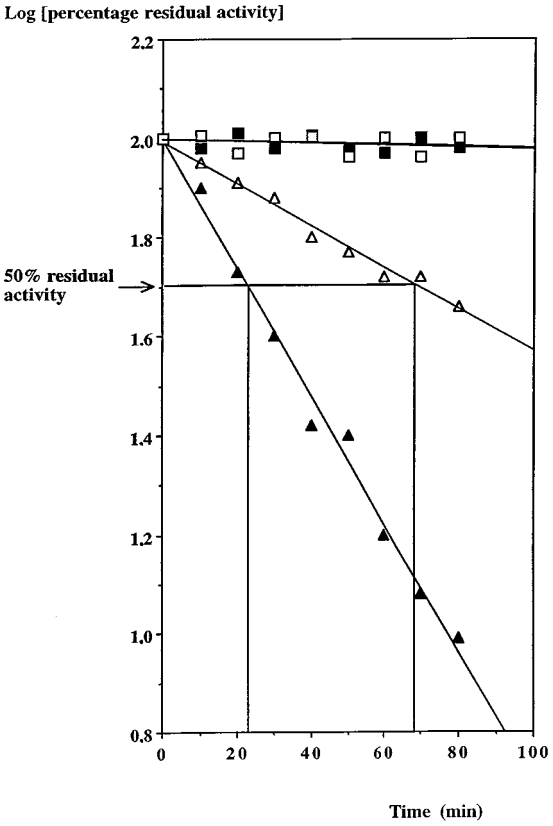

FIG. 4. Heat inactivation curves of native AspRS and the Pro555Ser-mutated enzyme for amino acid activation and acylation activities. Native AspRS (squares) and Pro555Ser (triangles) were incubated at 42°C in 50 mM Tris-HCl (pH 7.5)–30 mM KCl–1 mg of bovine serum albumin per ml. At various time intervals, aliquots were withdrawn and tested for acylation (dark squares and triangles) and amino acid activation activities (open squares and triangles) according to the procedures described in Materials and Methods.

measured apparent k_{cat} values have a more complex signification, in that they not only reflect the relative amounts of active and inactive molecules present but also may account for a possible effect of the mutation on the catalytic efficiency of the active species or for changes in a rate-limiting step, if one exists. From these results, it obviously may not be determined to which parameter change (k_{cat}, K_m, or both) inactivation of the mutated enzyme upon heating may be attributed. Whatever the explanation, the net result of the Pro555Ser mutation is to decrease the stability of the active configuration of both the amino acid activation and the tRNA acylation catalytic sites. It is worth noting that reducing agents such as β-mercaptoethanol did not protect the mutated AspRS against heat inactivation (data not shown), showing that the latter is not an oxidation-mediated process. Likewise, no protection was observed when the mutated enzyme was incubated at 42°C in the presence of $tRNA^{Asp}$, suggesting that tRNA does not strongly interact with regions destabilized by the Pro555Ser mutation. This is consistent with the fact that the Pro555Ser mutation had no effect on the $tRNA^{Asp}$ K_m value. Lastly, we observed (data not shown) that the growth rate of CS143 at 30°C is about twice as fast in standard LB medium as that in medium containing a low salt concentration (0.5 g of NaCl per liter). This effect of salt may be due to stabilization of the Pro555Ser functional conformation (and by consequence to an increase in the active enzyme molecules within the cell). However, no significant difference was observed between the inactivation rates of the purified mutated enzyme when heated in the presence of high or low salt concentrations (data not shown). A more likely explanation of this effect of salt relies on the fact that ions are strictly required for tRNA acylation catalysis. In the case of the *E. coli* aspartylation reaction, the optimal salt concentration is about 30 mM NaCl (7) (the low-salt LB medium contained only 8.5 mM). If it is considered, as may be reasonably assumed, that the level of functional AspRS molecules is limiting within CS143 at 42°C (due to the important inactivation rate of the Pro555Ser protein at that temperature), it seems clear that under these conditions the growth rate of CS143 must be sensitive to less-than-optimal salt concentrations. A second possibility is related to the fact that low levels of AspRS activity in vivo may significantly restrict protein synthesis, the consequences being limiting amounts of strategic proteins, decoding errors, or immature translation products. Thus, it may be that due to such dysfunctions, proteins playing a pivotal role in cell division became sensitive to ionic strength.

Structural interpretation of thermosensitivity. Sequence alignments of class II aaRS point to the functional importance of Pro555. This amino acid is one of the highly conserved residues characterizing motif 3 that is common to all class II aaRS (6) and which was shown to be involved in the active site organization of these enzymes (3). Moreover, the C-terminal region of AspRS, in which Pro555 maps, was shown to interact with the N-terminal part of the other subunit, thereby contributing to dimer stability (2, 4a). Studies of yeast AspRS concluded that the α2 conformation common to most class II aaRS is a prerequisite for the activities of these enzymes (5);

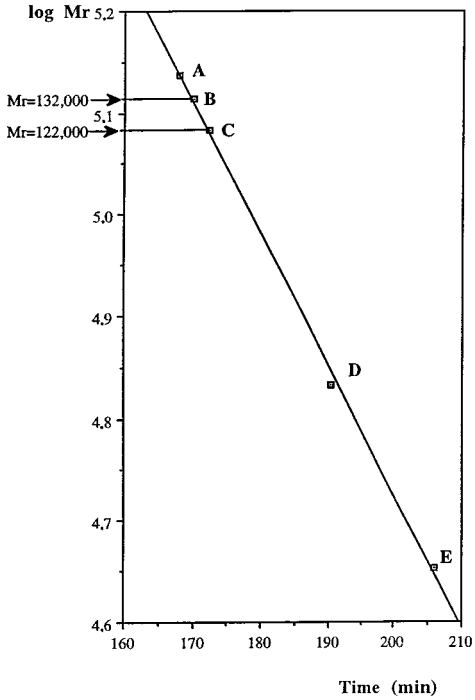

FIG. 5. Chromatographic behavior of the Pro555Ser enzyme on a gel filtration column. Elution of the HPLC gel filtration TSK3000 SW column (0.75 by 30 cm) was performed at 25°C by using a solution of 50 mM Tris-HCl (pH 7.5)–100 mM NaCl at a flow rate of 0.5 ml/min. The points on the calibration curve correspond to bovine serum albumin as dimer (M_r, 136,000) (A), Pro555Ser protein from *E. coli* (B), AspRS from *E. coli* (M_r, 122,000) (C), bovine serum albumin as monomer (M_r, 68,000) (D), and ovalbumin (M_r, 45,000) (E).

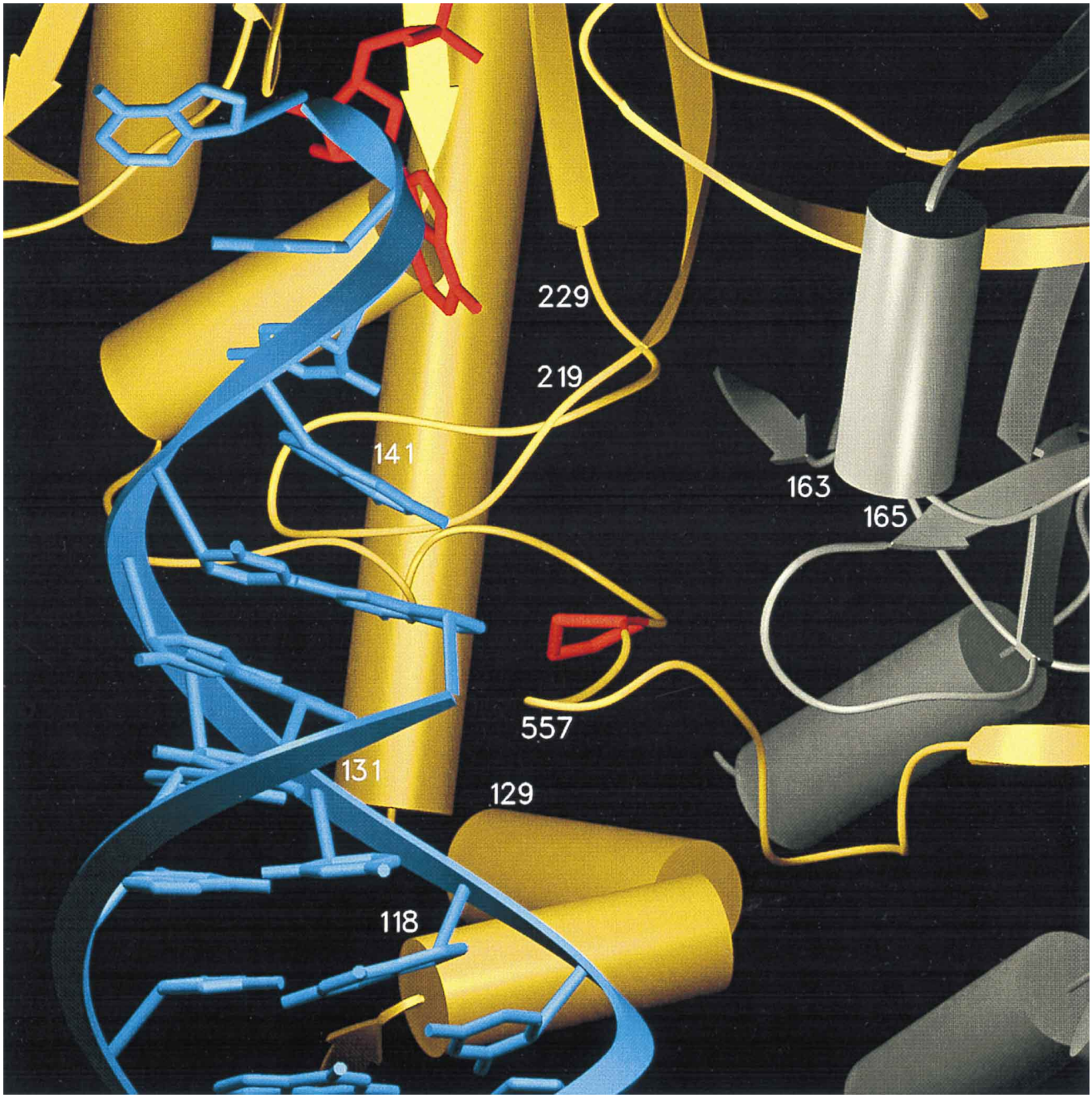

FIG. 6. Stereo view of the Pro555 region in the *E. coli* AspRS-tRNA^{Asp} complex. Blue, the tRNA molecule; gold, the protein; red, AMPPCP as well as Pro555; grey, AspRS from the other subunit. Distances are as follows: Pro555 to Pro555 (other monomer), 30 Å; Pro555 to AMPPCP (same monomer), 11 Å; and Pro555 to tRNA (same monomer), 9 Å.

structural constraints resulting from contacts at the interface subunits participate in the functional folding of the active center. Noticeably, deletion of five residues from the C terminus of yeast AspRS (comprising the Pro residue isosteric to Pro555 in *E. coli*) not only markedly affects acylation activity but also confers thermosensitivity to this enzyme (9). Taken together, these observations suggest that the Pro555Ser mutation impairs the integrity of structural elements directly or indirectly (via interface interactions) contributing to the stability of the enzyme active center. The existence of a significant structural change in the Pro555Ser mutation is supported by gel filtration analysis of a Pro555Ser-mutated protein with a TSK 3000 HPLC column. Figure 5 shows that the thermosensitive enzyme elutes from the column as a protein with an apparent molecular mass 10 kDa higher than that of the native enzyme. Noticeably, no appreciable difference was observed between the chromatographic behaviors of the 35% active and the completely heat-inactivated mutated enzymes, indicating that the observed conformational change had already occurred with the Pro555Ser mutation. The possibility that the change in structure is progressive until a major shift to a single inactive species occurs may be excluded. Indeed, in that case the active mate-

rial would be distributed over a broad band during elution. This was not observed, since fractionation of identical amounts of the 38% active and inactive mutated enzymes resulted in strictly identical absorbtion profiles (data not shown). The molecular bases of the critical role that Pro555 plays in the stability of the enzyme's catalytic center may tentatively be assessed from structural data of *E. coli* AspRS complexed with $tRNA^{Asp}$ and AMPPCP (2, 13a). The structure of the complex was determined by molecular replacement with the structure of the yeast-homologous complex as a starting model. It has been refined to an *r* value of 0.19 for data in the resolution range of 9 to 3.5 Å and without outliers in the Ramachandran diagram. It appears that within a distance of 10 Å, Pro555 is surrounded by four domains, three of which are from the same monomer and one of which is from the other subunit (Fig. 6). Inside the monomer, Pro555 is sandwiched between (i) a helix-loop-helix motif located in the hinge region residues 118 to 129 (a domain which links the N-terminal part of the protein to the C-terminal part and is involved in tRNA binding) and (ii) the central loop of motif 2 residues (221 to 229). At the back, Pro555 is in contact with residues 134 to 141, which are part of a long α-helix involved in AspRS dimerization. In the other subunit, Pro555 is very close to residues 163 to 165, which are located in a loop at the end of motif 1.

Key interactions include (i) residues located in the loop of motif 2 (the main chain of Gln226, which is less than 4 Å of Pro555, forms two H bonds with the adenosine of AMPPCP, an ATP analog [NH . . . N1 and CO . . . N6]) and (ii) residues located immediately after Pro555. The side chain of Lys556 binds to the main chain of Leu165 of the other subunit. Additional intrasubunit interactions occur between the protein and the tRNA; Thr557 binds to the phosphate backbone of U68 and Thr558 binds to U69. Any perturbation at this level, such as the Pro555Ser mutation, would certainly influence the local conformation.

It is reasonable to assume that the Pro555Ser mutation induces conformational modifications which might result in lower stability for the Lys556 and the Thr557 positions. One may hypothesize that after shifting to a stabler energy state, these residues would no longer be able to interact at the subunit interface or with the $tRNA^{Asp}$ acceptor helix. As mentioned above, changes at the dimer interface may impair the active site and consequently may be responsible for the thermosensitivity of the activation step. The loss of interactions with U68 and U69 seems the main factor responsible for abolition of the enzyme-charging capacity, enzyme contacts with the end of the acceptor stem being crucial for properly configuring the acylation transition state.

ACKNOWLEDGMENTS

We thank Professor G. Dirheimer for critical reading of the manuscript. The skillful technical assistance of M. L. Gangloff is gratefully acknowledged. We also thank A. Hoeft for oligonucleotide synthesis.

This work was supported by grants from the Centre National de la Recherche Scientifique, from the Medical Research Council and Science and Engineering Research Councils, and from the FEBS (Summer Fellowship).

REFERENCES

1. **Bachmann, B. J.** 1987. Derivations and genotypes of some mutant derivatives of *Escherichia coli* K-12, p. 1190–1219. *In* F. C. Neidhardt, J. L. Ingraham, K. B. Low, B. Magasanik, M. Schaechter, and H. E. Umbarger (ed.), *Escherichia coli* and *Salmonella typhimurium*: cellular and molecular biology, vol. 2. American Society for Microbiology, Washington, D.C.
2. **Boeglin, M., A. C. Dock-Bregeon, G. Eriani, J. Gangloff, M. Ruff, A. Poterszman, A. Mitschler, J. C. Thierry, and D. Moras.** 1996. Crystallization of *E. coli* aspartyl-tRNA synthetase in its free state and in a complex with *yeast* $tRNA^{Asp}$. Acta Crystallogr. Sect. D **52:**211–214.
3. **Cavarelli, J., G. Eriani, B. Rees, M. Ruff, M. Boeglin, A. Mitschler, F. Martin, J. Gangloff, J. C. Thierry, and D. Moras.** 1994. The active site of yeast aspartyl-tRNA synthetase: structural and functional aspects of the aminoacylation reaction. EMBO J. **13:**327–337.
4. **Cusack, S., C. Berthet-Colominas, M. Härtlein, N. Nassar, and R. Leberman.** 1990. A second class of synthetase structure revealed by X-ray analysis of *Escherichia coli* seryl-tRNA synthetase. Nature **347:**249–255.

4a. **Eiler, S., and D. Moras.** Personal communication.

5. **Eriani, G., J. Cavarelli, F. Martin, G. Dirheimer, D. Moras, and J. Gangloff.** 1993. Role of dimerization in yeast aspartyl-tRNA synthetase and importance of the class II invariant proline. Proc. Natl. Acad. Sci. USA **90:**10816–10820.
6. **Eriani, G., M. Delarue, O. Poch, J. Gangloff, and D. Moras.** 1990. Partition of tRNA synthetases into two classes based on mutually exclusive sets of sequence motifs. Nature **347:**203–206.
7. **Eriani, G., G. Dirheimer, and J. Gangloff.** 1990. Aspartyl-tRNA synthetase from *Escherichia coli*: cloning and characterization of the gene, homologies of its translated amino acid sequence with asparaginyl- and lysyl-tRNA synthetases. Nucleic Acids Res. **18:**7109–7117.
8. **Eriani, G., G. Dirheimer, and J. Gangloff.** 1990. Study of the structure-function relationship of arginyl-tRNA synthetase from *Escherichia coli*: isolation and characterization of the *argS* mutation MA 5002. Nucleic Acids Res. **18:**1475–1479.
9. **Eriani, G., G. Prévost, D. Kern, P. Vincendon, G. Dirheimer, and J. Gangloff.** 1991. Cytoplasmic aspartyl-tRNA synthetase from *Saccharomyces cerevisiae*. Study of its functional organisation by deletion analysis. Eur. J. Biochem. **200:**337–343.
10. **Hountondji, C., P. Dessen, and S. Blanquet.** 1986. Sequence similarities among the family of aminoacyl-tRNA synthetases. Biochimie **68:**1071–1078.
11. **Kast, P., C. Wehrli, and H. Hennecke.** 1991. Impaired affinity for phenylalanine in *Escherichia coli* phenylalanyl-transfer RNA synthetase mutant caused by Gly-to-Asp exchange in motif 2 of class-II transfer RNA synthetases. FEBS Lett. **293:**160–163.
12. **Lin, S. X., M. Baltzinger, and P. Remy.** 1983. Fast kinetic study of yeast phenylalanyl-tRNA synthetase. Biochemistry **22:**681–685.
13. **Mans, R. J., and G. D. Novelli.** 1961. Measurement of the incorporation of radioactive amino acids into proteins by a filter-paper disk method. Arch. Biochem. Biophys. **94:**48–53.

13a. **Moras, D., and S. Eiler.** Unpublished results.

14. **Rossmann, M. G., D. Moras, and K. W. Olsen.** 1974. Chemical and biological evolution of a nucleotide-binding protein. Nature **250:**194–199.
15. **Ruff, M., S. Krishnaswamy, M. Boeglin, A. Poterszman, A. Mitschler, A. Podjarny, B. Rees, J.-C. Thierry, and D. Moras.** 1991. Class II aminoacyl transfer RNA synthetases: crystal structure of *yeast* aspartyl-tRNA synthetase complexed with $tRNA^{Asp}$. Science **252:**1682–1689.
16. **Sharples, G. J., and R. G. Lloyd.** 1991. Location of a mutation in the aspartyl-tRNA synthetase gene of *E. coli* K-12. Mutat. Res. **264:**93–96.
17. **Shurvinton, C. E., R. G. Lloyd, F. E. Benson, and P. V. Attfield.** 1984. Genetic analysis and molecular cloning of the *Escherichia coli ruv* gene. Mol. Gen. Genet. **194:**322–329.
18. **Webster, T. A., H. Tsai, M. Kula, G. A. Mackie, and P. Schimmel.** 1984. Specific sequence homology and three-dimensional structure of an aminoacyl tRNA synthetase. Science **226:**1315–1317.
19. **Willison, J. C., M. Härtlein, and R. Leberman.** 1995. Isolation and characterization of an *E. coli* seryl-tRNA synthetase mutant with a large increase in K_m for serine. J. Bacteriol. **177:**3347–3350.